

# MEASUREMENTS OF HORIZONTAL FLOWS IN 1.6 $\mu\text{m}$ GRANULATION

TRON A. DARVANN

*Institute of Theoretical Astrophysics, University of Oslo,  
P. O.Box 1029 Blindern, N-0315 Oslo, Norway*

and

*National Solar Observatory,\* Sunspot, NM 88349, U.S.A.*

**Abstract.** We report on a first analysis of the horizontal motions in a 45 minute ( $32 \times 22$  arcsec<sup>2</sup> field of view) granulation time series (movie presented at the present IAU Symposium) obtained at 1.6  $\mu\text{m}$  with the Vacuum Tower Telescope (VTT) of the National Solar Observatory at Sacramento Peak (NSO/SP). High signal/noise flow maps are obtained by use of the local cross correlation technique (November 1986) which incorporates efficient attenuation of seeing and 5-min oscillations. The flow pattern, showing a ( $\approx 30$  arcsec diameter) supergranule with ( $\approx 8$ –15 arcsec) mesogranules superposed, is long lived compared to the 45 min of observations. The computed flows (velocity, divergence, vorticity) resemble the ones obtained at visible wavelengths (*e.g.*, by Brandt *et al.* 1991, November 1989, November and Simon 1988, Simon *et al.* 1988). The high quality of the the flow maps (due to a large number of selected images (1500), and (supposedly) smaller 5-min oscillations and better seeing conditions at 1.6  $\mu\text{m}$ ) allows us to study time evolution (resolution  $\approx 15$  min) of the details of the flow (spatial resolution  $\approx 3$  arcsec). An interesting new finding is the short lifetime ( $< 45$  min) of vorticity as opposed to the long lived ( $\gg 45$  min) divergence of the flow. Our study demonstrates the possibility of using the 1.6  $\mu\text{m}$  window to the opacity minimum region to study the horizontal flows at these deep layers of the photosphere.

**Key words:** infrared: stars – Sun: granulation – Sun: photosphere

## 1. Introduction

The technique of local cross correlation of granulation has been developed during the last few years to the point where it is a trusted and highly accurate tool for measuring horizontal flow patterns in the photosphere (November 1986, Simon *et al.* 1988). The method has been used in several investigations of the solar convection (Brandt *et al.* 1991, Müller *et al.* 1990, November 1989, Simon *et al.* 1988, Title *et al.* 1986, 1987, 1989). Flow patterns can be studied in detail, and *e.g.*, the flow divergence gives a proxy for vertical flow, while test particle (“cork”) simulations demonstrate the redistribution of magnetic flux by the convection. However, only presently, with greatly increasing data acquisition rates and computer capacity, the full power of the technique is starting to be seen, when applied together with other diagnostics *e.g.*, obtained from simultaneous multi-wavelength data (*e.g.*, Yi 1992). Particularly interesting is a *simultaneous* measurement of both small and large scale (from granular to global scale) flows for a study of interaction between different convective scales, and between convection and differential rotation (Darvann 1991), by observing granulation proper motion over a very large field of view. Noise limitations have been studied by November and Simon (1988), demonstrating that noise ( $\approx 100 \text{ m s}^{-1}$ ) from random granular motions dominate in a typical 1-hour average flow map, while seeing and 5-min oscillations contribute negligibly. Darvann (1991) showed that the noise level may be significantly further reduced by averaging over

\* Operated by the Association of Universities for Research in Astronomy, Inc. (AURA) under cooperative agreement with the National Science Foundation.

a much longer time than a couple of hours. While all the work up to now has been carried out at visible wavelengths, some gain in signal to noise ratio for the flow measurement might possibly be achieved at  $1.6 \mu\text{m}$ , thereby allowing smaller velocities to be detected. Granular velocities are larger at this wavelength (Keil 1980), and contrast is lower, but seeing and 5-min oscillations both have smaller amplitude. We present here a first computation of the topology of the flow at this wavelength. Keil *et al.* (1993, these proceedings) have obtained high resolution time series obtained in the visible and IR *strictly simultaneously*, and such a data set should be able to show the detailed differences of the flow topology, in addition to the signal/noise properties, between the two wavelengths.

## 2. Observations and Preprocessing

The observations were carried out on April 19, 1988 with the Vacuum Tower Telescope (VTT) at NSO/SP. The CHIRP image processing system was used in order to digitize and flatfield the granulation frames from a Vidicon IR video camera at a 1 Hz rate with subsequent recording on video tape. Visual image selection was thereafter carried out on a time series of 45 min duration showing variable, fair seeing conditions. The selection resulted in 1500 images approximately evenly spaced in time ( $\Delta t \approx 1.8 \text{ s}$ ). The time series was thereafter correlation tracked by an FFT method (von der Lühse 1983) in order to remove image motion. Images were also “brushed” (high gradient “bad” pixels removed, November 1986) and Fourier filtered to remove bad video lines that sometimes moved across the images. Figure 1b shows one of the images used for the measurement of horizontal flows.

## 3. Proper Motion Maps of Infrared Granulation

Proper motion maps were computed by local cross correlation (November 1986, Darvann 1991) of the 1500 image pairs (Fig 1b) and were noise-optimized through the technique of temporal summation of cross correlation functions (November and Simon 1988). Noise was further reduced by averaging results from 3 different computations applying three different correlation time lags (= the time difference between the correlated images in a pair); 50, 52 and 54 s, respectively. Figure 2 shows the average proper motion map (represented by the flow vectors) for the full 45 minute time series. The maximum speed is  $900 \text{ m s}^{-1}$ , RMS speed is  $300 \text{ m s}^{-1}$ , estimated accuracy  $\pm 100 \text{ m s}^{-1}$ . The effective spatial resolution of the map is determined by the Gaussian correlation window of 3.8 arcsec FWHM used in the computation.

A strong outflow with spatial scale corresponding to a little less than the typical size of a supergranule is evident near the center of the  $32 \times 22 \text{ arcsec}^2$  field of view. The outline of the “supergranule boundary” becomes more evident to the eye by computing the paths of evenly distributed “test particles” or “corks” moving with the flow (Simon *et al.* 1988). In Figure 2 we have allowed the corks (+ signs in the plot) to move for 8 hours in order to get an impression of the location of the “supergranulation network” for the 45 min average. The corks avoid regions of positive divergence (“outflow”), as shown in Figure 10 in the review paper by Koutchmy (elsewhere in these proceedings), and concentrates in the regions of neg-

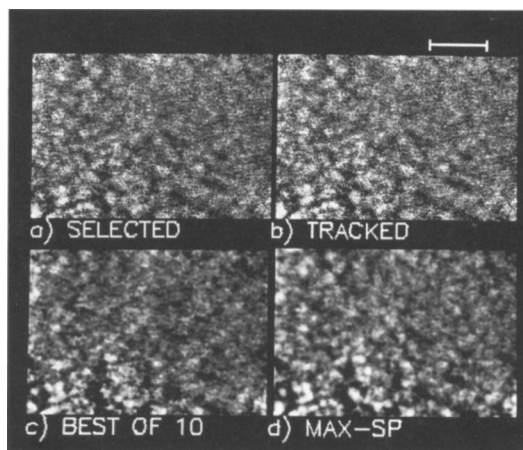


Fig. 1. Example of a single frame of the movie comparing image quality after 4 steps of processing have been applied. Length of the bar showing the scale is 7 arcsec. Difference in contrast and amount of detail between upper right and lower left of each frame is due to variations in sensitivity of the IR chip. *a*) Images after visual selection, filtering and “brushing.” *b*) Images after correlation tracking. This is the type of image used for the computation of horizontal motions. *c*) Best (highest RMS intensity) images out of every 10 images, subsequently smoothed by  $3 \times 3$  pixel bilinear interpolation. *d*) Images reconstructed from groups of 10 sequential images by use of spatial power maximization (MaxSP) (Koutchmy and Koutchmy 1989), smoothed by  $3 \times 3$  pixel bilinear interpolation. A movie shows a large improvement by MaxSP in terms of sharpness and stability.

ative divergence (“downflow”). The local extrema of divergence (typically  $\pm 3 \times 10^{-4} \text{ s}^{-1}$ ) may be interpreted to represent mesogranules (November and Simon 1988). The contours in Figure 2 show the vorticity averaged over the same 45 minute observing period.

A very useful evaluation of the quality of a flow map (complementary to noise estimation by temporal power spectral analysis of flow maps, November and Simon 1988), is to compare maps computed from different independent subsets of the data. For our data set, we computed a time series of 16 independent 2.8-min maps (90 image pairs contributing to each). From these maps we formed an “ODD” average map by averaging the 8 *odd* “interlaced” maps, and an “EVEN” average by averaging the 8 *even* ones. The ODD and EVEN maps (the divergences of which are shown in the bottom two figures of Figure 3) in this way become independent in terms of seeing (no common image pairs), and also almost independent in terms of granulation noise (2.8 min is a large fraction of the granulation lifetime, so that different granulation “realizations” contribute to the two maps). The correlation coefficients are high (0.7–0.8) (Table I), demonstrating the high quality of the computation. In a similar fashion, we averaged the 8 *first* 2.8 min maps to form a “FIRST” 22.5 min average map, and the 8 *last* 2.8 min maps to form a “SECOND” (later in time) 22.5 min map (the divergence of these are shown in the top two figures of Figure 3). Table I shows that correlation coefficients are high also in this case (0.5–0.6),

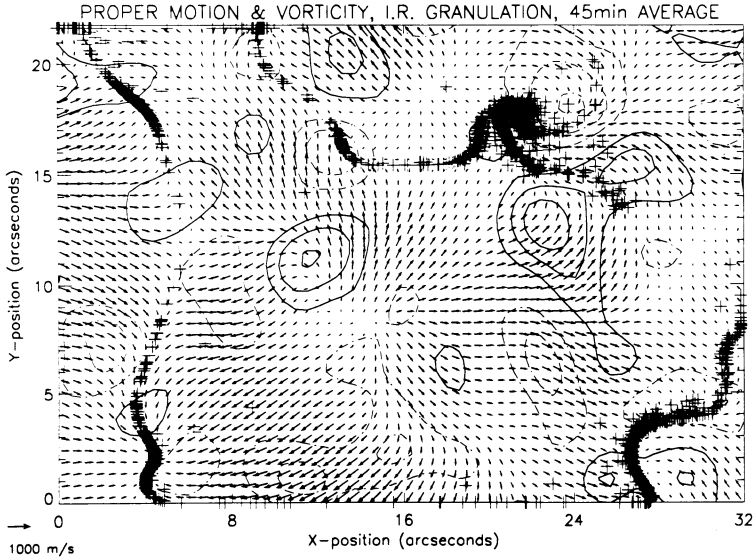


Fig. 2. A 45 min average proper motion map (flow vectors). Note the  $1 \text{ km s}^{-1}$  calibration flow vector to the lower left. Contours show flow vorticity (solid contour is positive (counterclockwise) vorticity, dashed contour negative (clockwise)), + -signs locate "corks" that have followed the flow vectors for 8 hours after initiating as an evenly distributed cork field at time 0. The same flow map, but with contours of divergence, is shown in Figure 10 of the review paper by Koutchmy elsewhere in these proceedings. Contour interval is  $1 \times 10^{-4} \text{ s}^{-1}$  for both figures; the zero-contour is not shown.

TABLE I

Correlation coefficient for comparison between the horizontal flow in the first (subscript 1) and second (subscript 2) 22.5 min average maps, and between the even (subscript EV) and odd (subscript ODD) maps (see the text). The correlation is given separately for the x- and y-component of the flow ( $v_x, v_y$ ), and the correlated divergence (DIV) maps are the ones shown in Figure 3. VOR denotes vorticity maps.

	$v_{x,1}$	$v_{y,1}$	DIV <sub>1</sub>	VOR <sub>1</sub>	$v_{x,EV}$	$v_{y,EV}$	DIV <sub>EV</sub>	VOR <sub>EV</sub>
$v_{x,2}$	0.65				0.82			
$v_{y,2}$		0.56				0.72		
DIV <sub>2</sub>			0.50				0.70	
VOR <sub>2</sub>				0.07				0.44
$v_{x,ODD}$								
$v_{y,ODD}$								
DIV <sub>ODD</sub>								
VOR <sub>ODD</sub>								

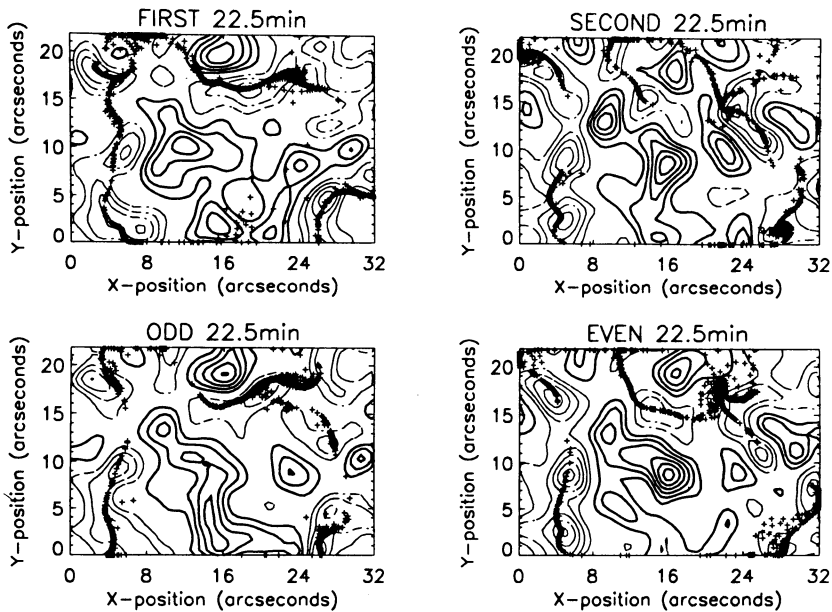


Fig. 3. Four divergence maps overlaid with cork positions after 8 hours, solid contour is positive divergence (“upflow”), dashed contours represent negative divergence (“downflow”). Upper two maps show the first and last 22.5 hr divergence maps making up the 45 min average shown in Fig 2. Lower two maps are 45 min maps composed by averaging odd and even (“interlaced”) 3 min maps. The large similarity (see Table I) between the four maps demonstrates the low noise level of the measurement.

but slightly lower than for the ODD/EVEN comparison, and we interpret this to be due to a slow evolution of a long lived flow pattern. The corresponding drop in correlation coefficient for the divergence is similar (Table I). For the vorticity, however, there is a dramatic decrease in correlation, and apparently the “lifetime” of vorticity must be very short compared to the “lifetime” of the divergence. Flow maps influenced by seeing has a tendency to show large values of vorticity, but the relatively large correlation (0.44) between the ODD and EVEN vorticity maps, rules out seeing noise as an explanation. Previous (white light) data sets that we have worked with also show a slight tendency for somewhat shorter “lifetime” of vorticity compared to divergence, but not at all as dramatic as in the present case. A time series of three 15 min average vorticity maps reveals large changes, and in some locations we see reversal of sign in the course of 45 min, leading one to think of torsional waves (see Koutchmy’s review paper in these proceedings).

We can also note here that the best way of qualitatively checking a flow map is to study an accelerated movie of the granulation. We were able to draw a map by hand that shows quite similar large scale features as the computed one.

#### 4. Conclusions

We have demonstrated that it is now possible to obtain high quality time series of granulation proper motion maps using local cross correlation of  $1.6 \mu\text{m}$  granulation images. Our preliminary study shows flow properties (flow amplitude, size scale of flow patterns etc.) that are within the range found by previous measurements in the visible. One possible exception is the apparent short lifetime of the flow vorticity (on a mesogranular scale); this needs to be investigated by temporal power spectral analysis. In order to detect smaller differences between the flows in the visible and IR, it will be necessary to carry out a statistical analysis of data obtained *strictly simultaneously* like the observations by Keil *et al.* (1993, these proceedings). Also, a larger field of view than presently obtained, would be of great value.

#### Acknowledgements

Travel support from ITA, Oslo, and Institute d'Astrophysique, Paris, is gratefully acknowledged. I would like to thank NSO/SP for the hospitality and outstanding working conditions offered to me during several visits, and for financial support in connection with attending the IAU Symposium. The present work has benefitted greatly from the never ending supply of inspiration and excellent observations provided by Dr. Serge Koutchmy. The software for proper motion measurements has been developed by Dr. Larry November. Fritz Stauffer programmed CHIRP, and Larry Wilkins provided electronics for the IR camera.

#### References

- Brandt, P.N., Ferguson, S., Scharmer, G.B., Shine, R.A., Tarbell, T.D., Title, A.M., Topka, K.: 1991, *Astron. Astrophys.* **241**, 219.
- Darvann, T.A.: 1991, Cand. Scient. Thesis, Univ. Oslo.
- Keil, S.L.: 1980, *Ap.J.* **237**, 1024.
- Keil, S.L., Kuhn, J.R., Lin, H., Reardon, K.: 1993, these proceedings.
- Koutchmy, S.: 1993, these proceedings.
- Koutchmy, O., Koutchmy, S.: 1989, in O. von der Lhe (ed.), *High Resolution Solar Observations*, National Solar Observatory, p. 217.
- Muller, R., Roudier, Th., Vigneau, J., Frank, Z., Shine, R., Tarbell, T., Title, A., Simon, G.W.: 1990, in L. Dezso (ed.), *The Dynamic Sun*, Debrecen, p. 44.
- November, L.J.: 1986, *Appl. Opt.* **25**, 391.
- November, L.J.: 1989, *Ap. J.* **344**, 494.
- November, L.J., Simon, G.W.: 1988, *Ap. J.* **333**, 427.
- Simon, G.W., Title, A.M., Topka, K.P., Tarbell, T.D., Shine R.A., Ferguson, S.H., Zirin, H., and The SOUP Team: 1988, *Ap. J.* **327**, 964.
- Title, A.M., Tarbell, T.D., Simon, G.W., and the SOUP Team: 1986, *Adv. Space Res.* **6**, 253.
- Title, A.M., Tarbell, T.D., Topka, K.P.: 1987, *Ap. J.* **317**, 892.
- Title, A.M., Tarbell, T.D., Topka, K.P., Ferguson, S.H., Shine, R.A., and the SOUP Team: 1989, *Ap. J.* **336**, 475.
- von der Lhe, O.: 1983, *Astron. Astrophys.* **119**, 85.
- Yi, Z.: 1992, *Quiescent Filaments, Magnetic Field, and Flows in the Photosphere*, Chapter 4 of Ph.D. Thesis, Univ. Oslo.